On incidence-dependent management strategies against a SEIRS epidemic: extinction of the epidemic using Allee effect

Tri Nguyen-Huu[1], Pierre Auger[2], and Moussaoui Ali[3]

[1]Institut de recherche pour le developpement
[2]IRD
[3]University of Tlemcen, Faculty of Sciences, Department of Mathematics

July 13, 2022

Abstract

We develop a mathematical model to study the effects of non-pharmaceutical interventions (NPIs) on the dynamics of an epidemic. The level of intervention is assessed as a fraction of the population being isolated and depends on the level of incidence of the epidemic in the population. We perform the mathematical analysis of the model and show that, depending on the choice of the prevalence-dependent isolation function, it is possible to create new endemic equilibria and to change the stability of the disease-free equilibrium for which the epidemic vanishes. The model is then applied to the case of the covid-19 pandemic. Several NPI management strategies are considered. In the case of a NPI intensity increasing with the level of infection, it is possible to avoid the initial epidemic peak of great amplitude that would have occurred without intervention and to stabilize the epidemic at a chosen and sufficiently low endemic level. In the case of a NPI intensity decreasing with the level of infection, the epidemic can be driven to extinction by generating an "Allee" effect: when the incidence is below a given level, the epidemic goes extinct while above it, the epidemic will still be able take hold at a lower endemic level. Simulations illustrate that appropriate NPIs could make the Covid-19 vanish relatively fast. We show that in the context of the covid-19 pandemic, most countries have not chosen to use the most efficient strategies.

Hosted file

`M2AS.tex` available at https://authorea.com/users/494902/articles/576809-on-incidence-dependent-management-strategies-against-a-seirs-epidemic-extinction-of-the-epidemic-using-allee-effect

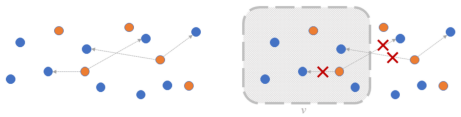

(a) Without NPI **(b)** With NPI

FIGURE 1 Reduction of the number of infections due to NPI. Infected individuals are represented in blue, and symptomatic/presymptomatic in orange. (a) Without NPI, four infections occur. (b) With NPI, a proportion $v = 0.5$ of individuals is isolated (shaded area). The number of infection is reduced to $(1 - v)^2 = 0.25$ of the number of original number of infections.

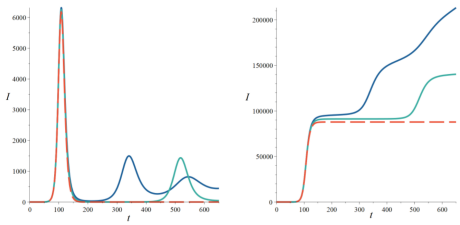

(a) Active cases **(b)** Cumulative cases (including reinfections)

FIGURE 2 Evolution of the epidemic in the absence of NPI $\upsilon = 0$, for $1/\gamma = 200$ (blue), 400 (green) and compared to a model without reinfection ($\gamma = 0$, red dashed curve). (a) active cases per 100,000 (b) and cumulative cases per 100,000. The initial conditions is ($S(0) = N - 1$, $E(0) = 0$, $I(0) = 1$). Parameters values are $\beta = 1.2$, $k = 0.27$, and $\alpha = 0.67$.

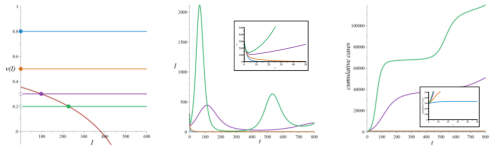

(a) Functions v and $\hat{v}$ **(b)** Number of active cases (I) **(c)** Cumulative cases

FIGURE 3 Comparison of constant control strategies: $v = 0.8$ (blue), $v = 0.5$ (orange), $v = 0.3$ (purple), $v = 0.2$ (green). Parameters values are $\beta = 1.2$, $k = 0.2$, $\alpha = 0.5$ and $\gamma = 1/200$, $N = 50{,}000{,}000$. The initial condition is I(0)=300 per 100,000. (a) comparison of functions v and $\hat{v}$, with stable (solid circles) and unstable (empty circles) equilibria. (b) evolution of the number of active cases I. An insert show the details of the region $0 < t < 50$. (c) Evolution of the number of cumulative cases.

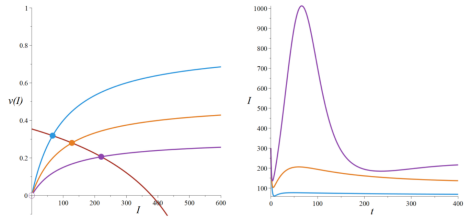

(a) Functions υ and $\hat{\upsilon}$ **(b)** Number of active cases (I)

FIGURE 4 Comparison of strategies lowering the endemic equilibrium. Chosen functions are $\upsilon : I \mapsto \upsilon_0 I/(I + 100)$, with $\upsilon_0 = 0.8$ (blue), $\upsilon_0 = 0.5$ (orange) and $\upsilon_0 = 0.3$ (purple). Parameters values are $\beta = 1.2$, $k = 0.2$, $\alpha = 0.5$ and $\gamma = 1/200$. The initial condition is I(0)=300 per 100,000 individuals. (a) comparison of functions υ and $\hat{\upsilon}$, with stable endemic equilibria (solid circles), and an unstable DFE (empty circle). (b) evolution of the number of active cases I per 100,000 individuals.

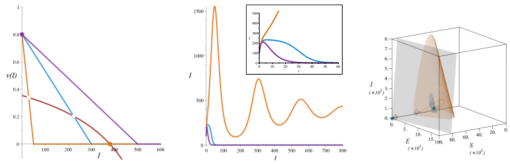

(a) Functions υ and $\hat{\upsilon}$ **(b)** Number of active cases (I) **(c)** Phase portrait

FIGURE 5 Comparison of control strategies which create an Allee effect. Chosen functions are piecewise linear maps, decreasing from 0.8 to 0 from $I = 0$ to $I = I_{max}$ and equal to 0 elsewhere, with $I_{max} = 300$ (blue), $I_{max} = 50$ (orange) and $I_{max} = 500$ (purple). Parameters values are $\beta = 1.2$, $k = 0.2$, $\alpha = 0.5$ and $\gamma = 1/200$, for a population of 50,000,000 individuals. The initial conditions is $S_0 = 60{,}000$, $E_0 = 800$, $I_0 = 100$ for 100,000 individuals. (a) comparison of functions υ and $\hat{\upsilon}$, with a stable (solid circle) DFE and unstable (empty circles) endemic equilibria. (b) evolution of the number of active cases I. The early dynamics is depicted in insert. (c) Phase portrait. Stable equilibria are represented by a solid sphere, and unstable equilibria by a diamond, in colors corresponding to their respective maps υ. Surfaces indicate the basin of attractions of the stable endemic equilibrium, the colors corresponding to their respective maps. The grey plane delimits the volume of possible initial conditions ($S + E + I + R \leq N$).

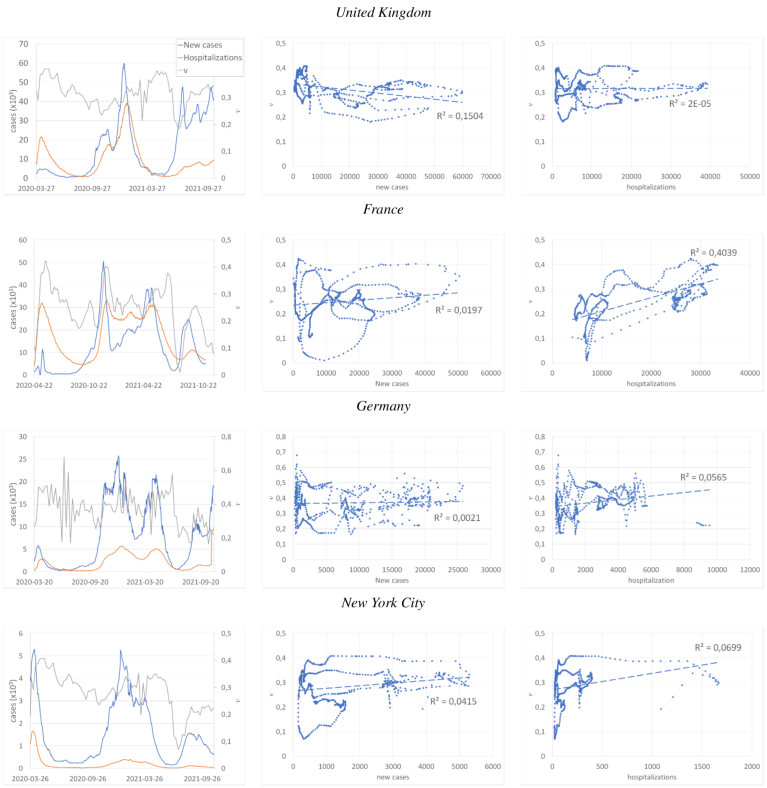

FIGURE 6 Epidemiological dynamics and NPI strategies for UK, France, Germany and New-York City. Left: time evolution of the number of new cases, admission to hospitals, and NPI intensity ν. Middle: phase portrait of NPI intensity ν vs new cases. Right: phase portrait of NPI intensity ν vs hospitalizations. For each point clouds, a linear regression has been performed in order to see if a linear relationship could be exhibited.

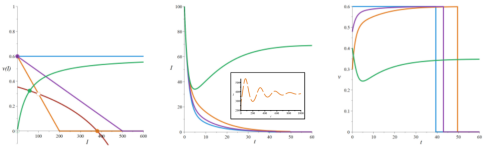

(a) Functions v and $\hat{v}$ **(b)** Number of active cases (I) **(c)** NPI intensity v

FIGURE 7 Comparison of the different NPI strategies: constant control (blue), decreasing function (purple and orange) and lower endemic equilibrium (green). Parameters values are $\beta = 1.2$, $k = 0.2$, $\alpha = 0.5$ and $\gamma = 1/200$, for a population of 50,000,000 individuals. The initial conditions is $I(0) = 100$ per 100,000. (a) comparison of functions v and $\hat{v}$, with stable (solid circles) and unstable (empty circles) equilibria. (b) evolution of the number of active cases I. Insert: an additional dynamic for the initial condition $S(0) = 45{,}000$, $E(0) = 200$, $I(0) = 800$ for the orange strategy. (c) NPI intensity $v(t)$.

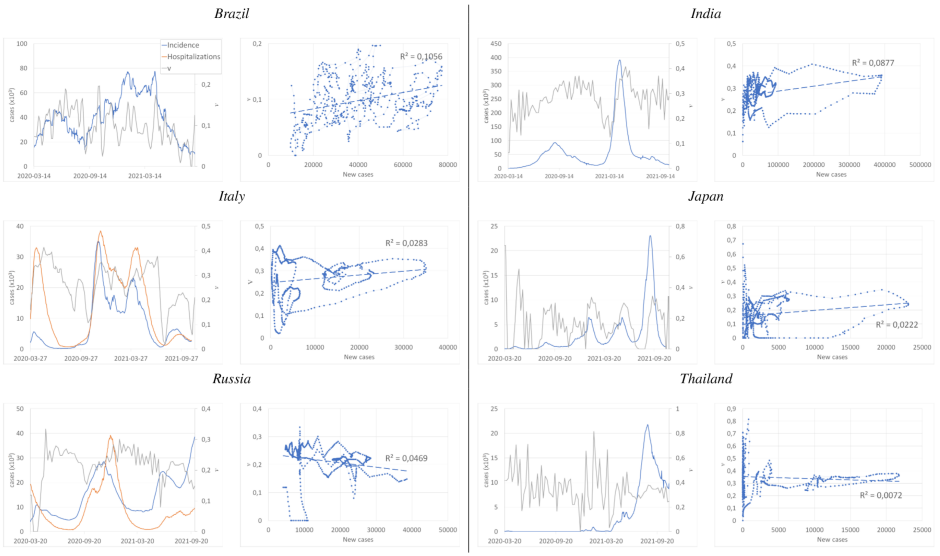

FIGURE 8 Epidemiological dynamics and NPI strategies for different countries. Left: time evolution of the number of new cases, admission to hospitals, and NPI intensity ν. Right: phase portrait of NPI intensity ν vs new cases. For the point cloud, a linear regression has been performed in order to see if a linear relationship could be exhibited.

Received: 00 Month 0000 | Revised: 00 Month 0000 | Accepted: 00 Month 0000

DOI: xxx/xxxx

ARTICLE TYPE

On incidence-dependent management strategies against a SEIRS epidemic: extinction of the epidemic using Allee effect

Tri Nguyen-Huu*[1,2] | Pierre Auger[1] | Ali Moussaoui[3]

[1]UMMISCO, Sorbonne Université, Institut de Recherche pour le Développement, Bondy, France
[2]IXXI, ENS Lyon, Lyon, France
[3]Laboratoire d'Analyse Non linéaire et Mathématiques Appliquées, Departement of Mathematics, Faculty of Sciences, University of Tlemcen, Tlemcen, Algeria

Correspondence
*Tri Nguyen-Huu, UMMISCO, Sorbonne Université, Institut de Recherche pour le Développement, IRD, F-93143 Bondy, France. Email: tri.nguyen-huu@ird.fr

Summary

We develop a mathematical model to study the effects of non-pharmaceutical interventions (NPIs) on the dynamics of an epidemic. The level of intervention is assessed as a fraction of the population being isolated and depends on the level of incidence of the epidemic in the population. We perform the mathematical analysis of the model and show that, depending on the choice of the prevalence-dependent isolation function, it is possible to create new endemic equilibria and to change the stability of the disease-free equilibrium for which the epidemic vanishes. The model is then applied to the case of the covid-19 pandemic. Several NPI management strategies are considered. In the case of a NPI intensity increasing with the level of infection, it is possible to avoid the initial epidemic peak of great amplitude that would have occurred without intervention and to stabilize the epidemic at a chosen and sufficiently low endemic level. In the case of a NPI intensity decreasing with the level of infection, the epidemic can be driven to extinction by generating an "Allee" effect: when the incidence is below a given level, the epidemic goes extinct while above it, the epidemic will still be able take hold at a lower endemic level. Simulations illustrate that appropriate NPIs could make the Covid-19 vanish relatively fast. We show that in the context of the covid-19 pandemic, most countries have not chosen to use the most efficient strategies.

KEYWORDS:
SEIRS, infectious dependent management of an epidemic, target endemic level, Allee effect, Covid-19.

1 | INTRODUCTION

We present here a theoretical approach aiming at evaluating the effects of some Non Pharmaceutical Interventions (NPI) such as lockdown, social distancing or teleworking in order to limit the number of cases. We discuss their ability to fulfill some requirements such as keeping the number of cases at a level low enough to be managed by hospitals, or maintaining a lockdown at a level low enough to avoid consequences that are too damaging to the economy. We are also looking for NPI measures in order to bring about the eradication of the epidemic. In SIRS and SEIRS classical epidemic models, there exist a disease free equilibrium (DFE) and a single endemic equilibrium (EE) which can be positive depending on the values of the parameters. A basic reproduction number of the epidemic $\mathcal{R}_0$ is defined and represents the number of people infected by a single infectious person during his illness. According to the value of this parameter, there are two cases. Either $\mathcal{R}_0$ is smaller than 1 and the

epidemic goes extinct, i.e. the DFE is globally stable while the EE does not exist, or else the epidemic takes hold, i.e. $\mathcal{R}_0$ is greater than 1, the DFE is unstable and the EE is globally stable.

The aim of this work is to propose NPI protection measures depending on the number of infected people to control and eradicate an epidemic. Therefore, a proportion of protected people is defined by function $\upsilon(I)$. Such infected dependent protection measures significantly allows modifying the global phase portrait by creating several endemic equilibria depending on the particular choice of the function $\upsilon(I)$. We will particularly consider choices of protection function which allow bringing about the extinction of the epidemic. In particular, we will focus on a class of protection functions which generate an "Allee" effect. The Allee effect is well known in population dynamics and ecology,[1]. The weak Allee effect keeps the population growth rate quite low but positive at low density, while the strong Allee effect induces a negative growth rate below a certain threshold,[2],[3]. The latter corresponds to a situation where the population goes extinct when its density is below the threshold. The Allee effect is aimed to take into account the difficulties for mating, or still the absence of cooperative behavior between individuals at low density causing the eradication of the species. In order to grow, the initial population must be at a sufficiently high density above this threshold. In the case of an harvested population, a high price of the resource due in particular to its scarcity can also induce an Allee effect[4]. Equivalently, such an effect could happen in epidemiology context, when the number of infected people is too small to start a wave of infection.

A judicious choice of functions $\upsilon(I)$ allows generating two endemic equilibria, one at a low level, denoted EE1, and the other at a higher endemic level denoted EE2. By analogy, the case where EE1 is unstable while EE2 is stable corresponds to an "Allee" effect. According to the basins of attraction of equilibria, we can create a situation where any initial condition chosen below the level of infection of EE1 can lead to the eradication of the epidemic whereas for any initial condition above, the epidemic settles and stabilizes in the long term at the level of EE2. In this work we focus on a class of functions $\upsilon(I)$ allowing to generate such an Allee effect as well as any other class of functions allowing to cause the extinction of the epidemic.

The article is made up of seven sections. After an introductory part, section 2 presents a general SEIRS epidemic model with infected dependent control, the mathematical analysis of the epidemic model, such as existence of endemic equilibria and stability properties. In section 3, we discuss the application of the model to the SARS-CoV-2 epidemic. In section 4, we compare several infection-dependent NPI strategies. Among these, we present a constant level strategy, a strategy to avoid a large-scale epidemic peak and to stabilize the epidemic at an endemic level low enough to avoid congestion in hospitals and strategies that allow generating an Allee effect which permits to provoke the extinction of the epidemic below some endemic threshold. Section 5 is devoted to identify which strategies have been used againts covid-19. Section 6 presents a discussion of the results with a comparison of the different strategies showing the advantages, limitations and costs of each one. We conclude in section 7.

2 | A SEIRS MODEL WITH NPI DEPENDING ON THE NUMBER OF INFECTED PEOPLE

In the following model, the population is distributed among four compartments which are almost equivalent to those of a classical SEIRS model: a compartment S with susceptible individuals, a compartment E with exposed individuals, a compartment I with both asymptomatic (infectious without symptoms onset) and pre-symptomatic (infectious before symptoms onset or test) individuals. A compartment R contains individuals that have been removed from the infection dynamics, i.e. asymptomatic individuals after recovery, and symptomatic individuals, who are assumed to be quarantined as soon as they get aware of their condition (symptoms onset or positive test). We assume a constant total population $N = S + E + I + R$ since the time scale of the epidemic is small compared to the one of population growth.

We consider an epidemic focus, such as a country where the epidemic has just started. It is normally necessary to take into account the urban mobility of individuals in the dynamics of the epidemic. We cite the work[5], in which aged structured individuals are supposed to move between their place of residence, workplaces, universities, schools, public places, shopping centers and more places,[6] and[7]. In a previous model[8], we also took into account the daily movements of people between their home and the various places where they are required to move and where they are more or less protected from contact with infectious persons as well as lockdown and protection by masks following the work by[9].

We assume individuals can switch between a normal state and a state in which they are removed from the dynamics because of NPI such as isolation, lockdown or social distancing. Thus NPI result in a proportion υ of the population being in the state of isolation. We emphasize on the fact that maintaining a proportion υ of the population in state of isolation does not mean that the population is separated in two groups (one group with individuals that stay in normal state, and the other with individuals that stay isolated), but that individuals can change state as long as this proportion remains constant. A NPI that imposes two days

of teleworking per labour week (five days) would result in a proportion $\upsilon = 40\%$ of isolated people working from home every day. However people may be in a different state every day. In the following sections, υ will refer to a more general definition of NPI intensity that will not only apply to lockdown or teleworking but also to social distancing or mask wearing, by assuming that any measure is equivalent to a percentage of time spent in isolation. It should be noticed that measures such as lockdown, stay-at-home or curfew apply to the whole population, independently of their infection status.

Infected individuals follow the natural process of the disease corresponding to a classical SEIRS model, i.e exposed individuals can become infected after an incubation time $\frac{1}{k}$. Infected individuals are removed after an average time $\frac{1}{\alpha}$, either because they recovered, or because they have been tested or are symptomatic, and thus quarantined. They lose their immunity after a time $\frac{1}{\gamma}$. The number of newly infected individuals per unit of time for the population in a classical SEIRS model is given by the expression $\beta\frac{SI}{N}$, where β is the transmission rate of the disease for one infectious individual in a population with only susceptible individuals. Since the same NPI rules apply to susceptible and asymptomatic/presymptomatic individuals, only a proportion $1-\upsilon$ of both S and I is involved in the disease transmission. Thus this expression must be replaced by $\beta\frac{(1-\upsilon)S(1-\upsilon)I}{N}$. Figure 1 illustrates the reduction of the number of infections: without NPI, four infections occur. With NPI, a proportion $\upsilon = 0.5$ of the population is isolated (shaded area) and cannot be infected or infect others. Compared to the case without NPI, infections can only occur between two persons outside of the shaded area, thus the ones with a red cross cannot occur anymore. The number of infection is reduced to $(1-\upsilon)^2 = 0.25$ of the original infections.

The modified SEIRS model reads

$$\begin{cases} \frac{dS}{dt} &= -\beta(1-\upsilon)^2\frac{SI}{N} + \gamma R, \\ \frac{dE}{dt} &= \beta(1-\upsilon)^2\frac{SI}{N} - kE, \\ \frac{dI}{dt} &= kE - \alpha I, \\ \frac{dR}{dt} &= \alpha I - \gamma R. \end{cases} \tag{1}$$

Individuals who present onsets or who have been tested are supposed to be definitively isolated and removed from the dynamics, thus belonging to the removed class R. To summarize, υ represents the proportion of isolated individuals for whom the status is unknown, while the isolation of individuals who have been recognized as infectious is part of the removal process corresponding to the term αI (see section 3.1 for more details on α). The parameters are summarized on Table 1 .

TABLE 1 Parameters used in model 1.

Parameter	Interpretation
β	infection rate
k	transfer rate from exposed to infected. $1/k$ is the average incubation duration.
α	$1/\alpha$ is the average time spent in the infectious state.
γ	transfer rate from recovered to susceptible. $1/\gamma$ is the average time before losing immunity.
υ	intensity of NPI, measured as the equivalent proportion of the population in isolation.

Now, let us consider effect of NPI which depend on the number of infected individuals, i.e. we impose that the proportion of individuals $\upsilon(I)$ in state 1 depends on the intensity of the epidemic, i.e. the number of infected individuals I.

Since the dynamics of R can be deduced from the ones of S, E and I, the dynamics is governed by the system

$$\begin{cases} \frac{dS}{dt} = -\beta(1-v(I))^2\frac{SI}{N} + \gamma(N-S-E-I), \\ \frac{dE}{dt} = \beta(1-v(I))^2\frac{SI}{N} - kE, \\ \frac{dI}{dt} = kE - \alpha I. \end{cases} \tag{2}$$

The resulting model is a SEIRS model with a modified transmission rate that reflects the NPI intensity which changes with the number of infected individuals. One way to derive the previous SEIRS model would also be to consider the version of the baseline confinement model in[8] and to assume that the proportion $v(I)$ of isolated people depends on the number of infected people I. However, the classical SEIRS models can only have one endemic equilibrium while the model with NPI can have several endemic equilibria and a different dynamics. The model obtained with constant v is similar to the one in[8].

2.1 | Disease Free Equilibria

In mathematical epidemiology, Disease Free Equilibria (DFE) are defined as equilibria for which no individual is infected by the disease, i.e. $I = E = 0$ in our model. Instability of the DFE usually corresponds to a value of the basic reproduction number $\mathcal{R}_0$ greater than 1 and is associated to the occurrence of an epidemic wave[10]. Equilibria of system 1 verify $\alpha I - \gamma R = 0$, which implies $R = 0$ at a DFE since $I = 0$. Finally $S = N - E - I - R = N$, which makes $(N, 0, 0)$ the unique Disease Free Equilibrium of model 2.

2.2 | Endemic equilibria

Interior endemic equilibria (S^*, E^*, I^*) verify:

$$\begin{cases} \beta(1-v(I^*))^2\frac{S^*I^*}{N} = \gamma(N-S^*-E^*-I^*), \\ \beta(1-v(I^*))^2\frac{S^*I^*}{N} = kE^*, \\ kE^* = \alpha I^*. \end{cases} \tag{3}$$

The equilibrium susceptible population can be expressed in terms of the infected one:

$$S^* = N - \left(1 + \frac{\alpha}{k} + \frac{\alpha}{\gamma}\right) I^*. \tag{4}$$

The infected population I^* verifies the following expression:

$$\frac{\beta}{N}(1-v(I^*))^2\left(N - \left(1 + \frac{\alpha}{k} + \frac{\alpha}{\gamma}\right) I^*\right) = \alpha. \tag{5}$$

Let us define the function $\hat{v}$ such that for $I \geq 0$,

$$\hat{v}(I) = 1 - \frac{1}{\sqrt{\mathcal{R}_0 - \frac{\beta}{N}\left(\frac{1}{\alpha} + \frac{1}{k} + \frac{1}{\gamma}\right) I}}. \tag{6}$$

where $\mathcal{R}_0 = \frac{\beta}{\alpha}$ is the basic reproduction rate of the SEIRS epidemic. We deduce from equation (5) that at endemic equilibria, the equality

$$v(I^*) = \hat{v}(I^*) \tag{7}$$

holds. For a given control function v associated to a given set of mitigation measures, the set of endemic equilibria can be determined by finding the solution of equation (7). In other words, each time that the graph of the chosen function v intersects the function $\hat{v}$, it corresponds to an endemic equilibrium, as it will be illustrated in the next section.

Function $\hat{v}$ is a monotonously decreasing function and intersects the abscesses axis at the classical endemic equilibrium $I_{EE} = \frac{\mathcal{R}_0 - 1}{\frac{\beta}{N}\left(\frac{1}{\alpha} + \frac{1}{k} + \frac{1}{\gamma}\right)}$, reached in absence of mitigation measures ($v = 0$). We also note that $\hat{v}(0) = 1 - \frac{1}{\sqrt{\mathcal{R}_0}}$. As shown in the following subsection, the disease free equilibrium (DFE) is stable if and only if $v(0) > 1 - \frac{1}{\sqrt{\mathcal{R}_0}}$.

2.3 | Stability analysis

We now study the dynamics of the SEIRS model by finding the stability of the equilibria (DFE and endemic equilibria). For the sake of simplicity, we assume that v is C^1 around the equilibria. The Jacobian matrix for the SEIRS Model (2) reads:

$$J = \begin{pmatrix} -\frac{\beta}{N}(1-v(I))^2 I - \gamma & -\gamma & -\frac{\beta}{N}(1-v(I))^2 S - \gamma + 2\frac{\beta}{N}v'(I)(1-v(I))IS \\ \frac{\beta}{N}(1-v(I))^2 I & -k & \frac{\beta}{N}(1-v(I))^2 S - 2\frac{\beta}{N}v'(I)(1-v(I))IS \\ 0 & k & -\alpha \end{pmatrix}. \tag{8}$$

2.3.1 | Local stability of the DFE

For the DFE, $(N, 0, 0)$, the Jacobian reads

$$J_{DFE} = \begin{pmatrix} -\gamma & -\gamma & -\gamma - \beta(1-v(0))^2 \\ 0 & -k & \beta(1-v(0))^2 \\ 0 & k & -\alpha \end{pmatrix}. \tag{9}$$

We are ensured to find one negative eigenvalues, $\lambda_1 = -\gamma < 0$. We consider the remaining minor matrix J_{MIN}:

$$J_{MIN} = \begin{pmatrix} -k & \beta(1-v(0))^2 \\ k & -\alpha \end{pmatrix}. \tag{10}$$

We find that its trace, $Tr(J_{MIN}) = -k - \alpha$ is negative and that the determinant, $det(J_{MIN}) = k(\alpha - \beta(1-v(0))^2)$ can be positive or negative. It is positive when $v(0) > 1 - \frac{1}{\sqrt{\mathcal{R}_0}}$. Under these conditions, the DFE is stable and it is possible to generate an Allee effect.

2.3.2 | Local stability for an endemic equilibrium

For any interior equilibrium (S^*, E^*, I^*), the Jacobian matrix simplifies by incorporating equilibrium expressions (3):

$$J^* = \begin{pmatrix} -\gamma - \frac{kE^*}{S^*} & -\gamma & -\gamma - \alpha + 2\frac{kv'(I^*)E^*}{(1-v(I^*))} \\ \frac{kE^*}{S^*} & -k & \alpha - 2\frac{kv'(I^*)E^*}{(1-v(I^*))} \\ 0 & k & -\alpha \end{pmatrix}. \tag{11}$$

The characteristic equation reads as follows:

$$\lambda^3 + a_1\lambda^2 + a_2\lambda + a_3 = 0, \tag{12}$$

with:

$$a_1 = \left(\alpha + k + \gamma + \frac{kE^*}{S^*}\right) > 0, \tag{13}$$

$$a_2 = (\alpha + k + \gamma)\frac{kE^*}{S^*} + \gamma(k+\alpha) + 2\frac{k^2 v'(I^*)E^*}{(1-v(I^*))}, \tag{14}$$

$$a_3 = 2\frac{\gamma k^2 v'(I^*)E^*}{(1-v(I^*))} + (\alpha\gamma + \gamma k + \alpha k)\frac{kE^*}{S^*} > 0. \tag{15}$$

The Routh-Hurwitz conditions $a_1 > 0$ and $a_3 > 0$ are always verified for a positive interior endemic equilibrium. If $v'(I^*) > 0$, it is easy to check that the last Routh-Hurwitz condition is also verified. Indeed, after simplification, $a_1 a_2 > a_3$ reads:

$$(\alpha^2 + k^2 + \gamma^2 + \alpha k + \alpha\gamma + k\gamma)\frac{kE^*}{S^*} + (\alpha + k + \gamma)\left(\frac{kE^*}{S^*}\right)^2 + \gamma(k+\alpha)\left(\alpha + k + \gamma + \frac{kE^*}{S^*}\right) + 2k^2\left(\alpha + k + \frac{kE^*}{S^*}\right)\frac{v'(I^*)E^*}{1-v(I^*)} > 0. \tag{16}$$

It is always verified for a positive endemic equilibrium when $v'(I^*) > 0$. In other words, if the level of protection increases with the number of infected individuals, the endemic equilibrium is stable. It is still true when $v'(I^*) < 0$ and $|v'(I^*)|$ is small. In other cases ($v'(I^*) < 0$ and $|v'(I^*)|$ is larger than a given threshold), the equilibrium is unstable.

As a consequence, the stability of endemic equilibria is independent of the stability of the DFE, and equilibria with the same stability can coexist.

2.4 | Numerical simulations

In the following sections, analytical results are supported by simulations. Simulations are performed in Maple using a Fehlberg fourth-fifth order Runge-Kutta numerical scheme (RKF45)[11]. For ODE systems in epidemiology, it is important to ensure that the numerical results are accurate and carry the qualitative properties of the solutions. Some studies focused on numerical methods dedicated to epidemiology, such as[12] or[13]. However, like other papers relying mostly on the analytical study of the systems (equilibria, stability, asymptotic dynamics) such as[14], we do not provide a complete proof of the convergence analysis (consistency, stability), as simulations are used mainly to illustrate the dynamics. All simulations outputs appear to be qualitatively consistent with the analytical results, as well as the numerical values (equilibria).

3 | APPLICATION TO THE COVID-19 EPIDEMIC

The onset of the Covid-19 epidemic was brutal with very high peaks of contamination leading to the saturation of intensive care units. In the United States, the occupancy rate of intensive care beds reached over 60% in the most populous states and large cities[15]. In France, the number of beds able to accommodate severely ill patients requiring intensive care in hospitals is limited to around 5,000 beds and the number of respirators available seemed also insufficient in view of the foreseeable arrival of seriously ill patients. In the absence of any measures, a very significant proportion of the population would have been infected after the epidemic wave. As a result, several governments in the world have decided to put in place NPI such as lockdown, social distancing or teleworking in order to limit the number of cases and keep hospital admissions of seriously ill patients below the hospital capacity threshold. This policy has been adopted by many countries and has worked with some success and limitations. Anyway hospitals were under very strong pressure leading sometimes to the saturation of intensive care units[16] despite such measures. The evaluation of the effects of NPIs is a central question which has been studied in previous works such as[17] in Italy, or in[14] where the authors evaluate how successful were the governmental measures in Rohingya Refugee Camps.

However, lockdown has had disastrous consequences for the economy, generating waves of unemployment, causing considerable budget deficits for the states, with very serious difficulties for those in need. Some countries have chosen to set up a partial lockdown while maintaining activity or have opted to end the lockdown early enough to limit the disastrous consequences for their economy, especially in Northern Europe. Many countries remain extremely cautious in this area, fearing the occurrence of successive epidemic waves after lockdown. The question of the end of lockdown is therefore crucial and it is important to develop scientific methods allowing to control this phase by limiting the damage.

NPI have been set up in order to rapidly address problems such as intensive care units overload and hospital pressure. However they were not specifically thought as a long term answer to a long lasting epidemic (several years), that may be caused by reinfection. It is commonly admitted that immunity usually lasts at least six months, but there is still uncertainty about a possible loss of immunity that would happen later on. As of today, a few cases of reinfection have been reported[18]. In[19], the author spots that reinfection is possible but the bigger question is "if reinfections are going to happen, how frequently are they happening?". In a preprint, Ward et al.[20] observe a decline of antibodies in UK patients, which led to a fear of a possible loss of immunity. Furthermore, the appearance of new variants also increases the possibility of reinfection[21,22].

3.1 | Dynamics without protection measures: parameters estimation based on Covid-19

Much work has been devoted to modeling the covid epidemic:[23,24,25] in China,[26,27,28] in Japan and in Algeria[29,30]. We also cite[31] in which the authors studied the effects of different quarantine and protection measures on the dynamics of the epidemic with a mathematical model, and[32] for Canada. Only a few works have been devoted to modelling the epidemic in the hypothesis of reinfection, such as[33] or[34].

The question of reinfection quickly rose with the onset of the pandemic, as it was unclear if immunity could be lost[35]. The loss of immunity or the risk of reinfection is an important question in epidemiology, as for HIV[36]. In the context of Covid-19, few cases of re-infections have been observed,[18], but most studies prior to fall 2021 suggested a long-lasting protection ($\geq$ 90 days,[37], $\geq$ 6 months[38]) but couldn't totally exclude the possibility of reinfections after a longer time or because of mutations. However, the appearance of new variants shed a light on massive reinfection occurrences. Evidences that variants could elude immune responses were found[21,22]. Several new variants (English, South African, Brazilian, Delta, Omicron) have been able to develop and even replace the original virus. These variants can be more virulent, more contagious and for some of them even more resistant to vaccines (see[39] for the Brazilian variant,[40] for UK and South Africa). It has been found recently that omicron

variant might evade antibodies induced by infection or vaccination[41]. In[42] it is suggested the relative risk of reinfection has risen to 81%. Long term reinfections due to new variants or loss of immunity have become a realistic hypothesis. In this general context, we consider a SEIRS model with the possibility of re-infection in the long term, with a reinfection rate γ. For the Covid 19 epidemic, we use the same general SEIRS model presented in the previous theoretical section. Since it is a highly simplified model which relies on strong assumptions, it may not be suitable for a realistic description or prediction of the current pandemic. However, it can provide useful qualitative information about the evolution of the disease in the context of possible re-infections, and about the benefits and disadvantages of different NPI strategies.

Parameters of the model can be estimated from various medical and statistical reports about Covid-19.

As of 2022, if the proportion of asymptomatic is pretty much well known (50% in[43], 40% in the meta-analysis performed in[44]), there is no clear consensus about the role of asymptomatic carriers on the dynamics of the population. Some studies account for more than half infections are due to asymptomatic carriers[45], while other suggest that asymptomatic transmission is marginal or due to a misclassification of presymptomatic cases as asymptomatic[46,47]. Because of those uncertainties, we do not take into account separate compartments for asymptomatic and symptomatic people in this work for the sake of simplicity. Instead we consider a class I which includes both symptomatic and presymptomatic carriers (Symptomatic carriers are included in the R class since they are supposed to be isolated as soon as they are aware of their condition). As a consequence, the average time spent in the infectious class $1/\alpha$ lies somewhere between the average infectious time for presymptomatic carriers $1/\alpha_p$ and the one for asymptomatic carriers $1/\alpha_a$, i.e. $1/\alpha \in [1/\alpha_p, 1/\alpha_a]$. It was found in[48] that infectiousness can occur from 2.3 days (95% CI, 0.8-3.0 days) before symptom onset, with a peak at 0.7 days (95% CI, 0.2–2.0 days) before onset. We estimate a rough lower boundary for $1/\alpha_p \geq 1$. The same study found a significant decline of infectiousness 10 days after onset. Other studies suggest that an infection more than 5 days after symptoms onset is very unlikely[49]. We thus set an upper boundary for $1/\alpha_a \leq 7.3$. As a consequence, we estimate that the parameter α lies in the interval $[0.13, 1]$.

As a consequence, we choose to set $\alpha = 0.67$ in this model. The model we obtain does not differ qualitatively from a model with an explicit asymptomatic compartment and provide a similar dynamic, with a marginal quantitative difference. On the contrary, such an approach allows avoiding the use of too many parameters on which there is a lot of uncertainty, thus following the principle of parsimony. Additional information obtained by using an asymptomatic compartment would have not be useful considering the scope of our study, and it would have come with a much higher prior uncertainty.

Following the estimation of α, we set parameter k to 0.27 day^{-1} since the average duration between infection and symptoms onset is 5.2 days[50].

$\mathcal{R}_0 = \frac{\beta}{\alpha}$ has been estimated between 2 and 6 for most countries, with most probable values in the range 2-3[51]. Some other studies suggest even higher values (between 3.5 and 6,[52]). In the following simulation, we decide to set $\beta = 1.2$ in order to obtain $\mathcal{R}_0 = 2.4$. In section 5, we will estimate β for each case study based on incidence time series obtained from data sources.

It is to be noted that estimates of the previous parameters (α, β, k) may be very inaccurate. In the case of Covid-19, one may find inconsistencies about indicators estimations between different studies: they depend on many factors (country, population density, local habits, culture, genetics), may vary in time (seasonal effects, new variants), or may be based on different protocols. Nevertheless, we have sought to make a reasonable choice of parameters among those found in the literature. If there may be much uncertainty about the numerical values that we obtain from simulations, the qualitative results are robust despite the inaccuracy of the parameters estimations.

Finally, there is a major uncertainty about parameter γ at the time being. The average duration after which immunity is lost is $1/\gamma$. Values between 60 and 365 are used in[33]. As of today, immunity is assumed to last at the very least 200 days, so we consider several possible values of $1/\gamma$ larger than 200.

Figure 2 compares several dynamics in the total absence of protective measures, for a country population of 50,000,000 individuals for different values of γ. In the absence of NPI ($\upsilon = 0$), the dynamics follows the one of a classical SEIRS model, tending towards the endemic equilibrium with decreasing oscillations. Note that it differs from the one of a classical SEIR model without reinfection ($\gamma = 0$, red dashed line curve). In the latter, the epidemic eventually vanishes after one wave of infection. Also note that there is very little differences between the first peaks for the different values of γ.

It is known that in the absence of any protective measure against the epidemic, a large proportion of the population is infected after the first peak, in a proportion ranging from 0.8 to almost the entire population depending on the value of $\mathcal{R}_0$,[29,53,25]. The aim of this work is precisely to show that by using adequate protective measures it is possible to greatly limit the level of infection and even to cause the disappearance of the epidemic in a relatively short time.

Figure 2 shows that considering different values for γ lead to the same qualitative dynamics. Despite the large range for γ, the amplitude of the first peak is similar, while the second one is shifted in time but has a similar amplitude (Figure 2 a). Reinfection naturally causes an infinite growth of the cumulative cases (Figure 2 b) that occurs by stages.

The number of active cases I per 100,000 at the equilibrium decreases with $1/\gamma$. However Figure 2 a illustrates that if no control measures are taken, it remains high for a large range of values. Whatever the value of parameter γ, the first epidemic peak is very high and it is essential to take protective measures to limit the number of cases and even to stop the epidemic quickly.

4 | POSSIBLE STRATEGIES AGAINST AN EPIDEMIC WITH REINFECTION

We now present several possible strategies to fight the epidemic when it starts. Based on the mathematical analysis of the general SEIRS model, we consider three main classes of epidemic NPI strategies: a first one consisting in a constant control, a second one stabilizing the epidemic at a sufficiently low target endemic level, a third one aiming at the eradication of the epidemic. In order to compare the various strategies, all simulations shown from now on use the same set of epidemiological parameters: $\beta = 1.2$, $k = 0.2$, $\alpha = 0.5$, $N = 50{,}000{,}000$ and $\gamma = 1/200$. All indicators (I, cumulative cases) are presented for 100,000 individuals to be consistent with indicators found in the literature.

4.1 | Strategy 1: constant control

We compare some constant control strategies with different intensities υ_0, shown in Figure 3 . The $\hat{\upsilon}(I)$ function is represented in red as in all the following figures. Each intersection with a constant υ function defines an endemic equilibrium, case of the purple and green function. Two outcomes are possible: if υ_0 is high enough, the epidemic goes extinct (Figure 3 b), since the DFE is stable and there is no endemic equilibrium ($\upsilon = 0.8$: blue and $\upsilon = 0.5$: orange, Figures 3 a). The number of active cases per 100,000 falls below 1 in around 80 days for $\upsilon = 0.5$ and around 20 days for $\upsilon = 0.8$. If υ_0 is low, the system tends towards a stable endemic equilibrium, since the DFE is unstable ($\upsilon = 0.3$: purple and $\upsilon = 0.2$: green). In the latter case, the number of active cases I shows oscillations and stabilizes around the endemic equilibrium. Peaks appear, corresponding to different waves of infection. As υ_0 increases, the value I^* at the equilibrium gets lower, peaks gets lower and more distant in time. The number of cumulative cases keeps increasing as people gets reinfected, its value eventually become larger than the total population.

4.2 | Strategy 2: NPI intensity increasing with the number of cases

This is the most natural strategy, since the intensity of measures usually increases with the level of epidemics. Many governments choose to have a light level of social distancing at low level of incidence, and more effective measures at higher levels.

The dynamics presents an unstable DFE and a unique endemic equilibrium. To illustrate this, we choose a family of increasing monotonic maps $\upsilon(I)$ $\upsilon : I \mapsto \upsilon_0 I/(I + 100)$ for different values of $\upsilon_0 = 0.8, 0.5$ and 0.3 (see Figure 4). The intersection with the curve $\hat{\upsilon}$ defines a unique endemic equilibrium I^* which is locally asymptotically stable. The value of I^* decreases with υ_0: I^* is respectively around 220, 128 and 67 for $\upsilon_0 = 0.3, 0.5$ and 0.8. High values of υ_0 lead to a rapid decrease of the epidemic, while a low value (purple curve) still allow large amplitude peaks, that may not be manageable by hospitals.

Since the number of cases decreases with the target endemic level, this strategy may turn useful to keep the epidemic low enough to prevent hospital congestion with a lower level of active cases. Unfortunately it is not possible to reach the extinction of the epidemic.

4.3 | Strategy 3: Seek to extinguish the epidemic

A necessary condition to end the epidemic is to have a stable DFE, which requires that $\upsilon(0) > \hat{\upsilon}(0)$. It requires a high NPI intensity at low level of cases I, contrary to strategy 2. This can be achieved by using any function $\upsilon > \hat{\upsilon}$, such as a sufficiently high constant control, as shown previously. A key element in our work is that since $\hat{\upsilon}$ is decreasing, it is much more important to keep υ at high levels when I is low than when I is high. Indeed, the extinction of the epidemic can be achieved with a decreasing function, with low intensity NPI when I is high, but high intensity NPI when I is low.

Figure 5 depicts the case of a decreasing control function υ (purple curve). Two other control functions (orange and blue) are represented, in order to see what would happen if the parameters were misevaluated. More specifically, we choose the following family of piecewise linear maps:

$$\upsilon : I \mapsto \begin{cases} \upsilon_0 \left(1 - \frac{I}{I_{max}}\right) & \text{if } 0 \leq I < I_{max}, \\ 0 & \text{if } I_{max} \leq I. \end{cases} \tag{17}$$

with $\upsilon_0 = 0.8$ and $I_{max} = 200$ (blue), 50 (orange) and 500 (purple) (see Figure 5 a).

The purple map drives the epidemic to extinction (Figure 5 b). Blue and orange maps create a lower unstable endemic equilibrium and a higher stable endemic equilibrium, generating an "Allee" effect: depending on the initial conditions, the epidemic may disappear or tend towards the high endemic equilibrium. The basins of attraction of the endemic equilibria for the different measures are represented in their respective colors in Figure 5 c. Stronger measures lead to smaller basin of attraction for the endemic equilibrium.

Such a strategy may be less natural since it means higher intensity measures when I is low than when I is high. However the intensity is still lower than in strategy 1, and it can provoke the extinction of the epidemic, what cannot be achieved with strategy 2. Furthermore, the extinction of the epidemic occurs in a relatively short time compared to the measures taken by most governments varying in intensity and which have been spread over more than a year.

5 | CASE OF THE COVID-19 PANDEMIC: ESTIMATION OF NPI INTENSITIES AND IDENTIFICATION OF THE STRATEGIES CHOSEN BY SEVERAL COUNTRIES

We now estimate the time evolution of NPI intensities $\nu(t)$ for several countries in order to find a match with one of the previous strategies discussed in the previous section. To that purpose, we use incidence (and equivalently the total number of new cases) and hospital admission (if available) data collected from John Hopkins University's Github repository and Our World in Data.

We simulate the evolution of the incidence using the SEIRS model defined in Section 2 using a time varying NPI intensity $\nu(t)$. Accordingly to Section 3.1, we use the following set of parameters: $\alpha = 0.67, k = 0.26, \gamma = 1/200$. We use the initial exponential phase of the epidemics to fit parameter β. During this initial phase, we assume that no NPI has been set up, hence $\nu(t) = 0$. We then estimate β by fitting the incidence curve obtained from the model with data using Least Square Method. We then assume that β is constant and that $\nu(t)$ evolves with time after the initial exponential phase. We use data time series from February 2020 and no later than October 2021 in order to avoid the effects of new variants like *delta* and *omicron* that would make the assumption of a constant β highly irrelevant. We then fit $\nu(t)$ week by week using Least Square Method and smooth the results by taking the mean over 7 days. We then intend to identify the strategies used by comparing the values of ν with the incidence and try to exhibit a tendency. Since incidence may be underestimated during the first wave of the epidemic, we also compare ν to the number of admissions in hospitals (when data is available), which is supposed to be a scaled and slightly shifted version of the real incidence curve. It then may provide a more reliable estimation of the real incidence rate, up to a multiplicative constant. Moreover, NPI were often set in order to avoid hospitals and ICUs saturation, which also makes this indicator more relevant than observed incidence. Figure 6 show the results obtained for United Kingdom, France, Germany and New York City. This figure shows time evolution of new cases, hospitalizations and $\nu(t)$, as well as the phase portraits ν vs *new cases* and ν vs *hospitalizations*. Results for a few other countries are shown in Appendix. Note that we replaced the incidence rate by the number of new cases, which is just a scaled version which is of the same order than hospitalization number, which makes the figure easier to read.

It appears that NPI intensity is not highly linearly correlated to new cases or hospitalization, apart from France ($R^2 = 0.40$), which could be associated to Strategy 2. For other countries, the value of ν appears to be relatively constant with the new cases or hospitalizations, hence they can be associated to Strategy 1. Other countries shown in appendix exhibit a constant or slightly increasing tendency, except for Russia, which exhibits a slightly decreasing tendency, which can be considered as constant. For United Kingdom, ν seems to slightly decrease with the number of cases, but is constant with hospitalizations, which certainly illustrates that hospitalization works better than the measured incidence rate.

All those examples illustrate that strategies 1 and 2 appear to be more natural than strategy 3, and thus are chosen by most countries.

6 | COMPARISON AND DISCUSSION OF THE EFFECTS OF VARIOUS NPI STRATEGIES ON THE DYNAMICS OF THE EPIDEMIC

We have shown that we can control an epidemic when it starts by imposing a level of NPI which depends on the number of infected persons each day. In the absence of protective measures, a peak of infected cases reaches over 6,000 cases per 100,000 and lasts for around 150 days. We now compare the different strategies to control the epidemic: strategies 1 (blue), 2 (green) and 3 (purple and orange), see Figure 7 a. All strategies have the same maximum intensity $\upsilon_0 = 0.6$. Blue and purple always cause the epidemic to end since the only equilibrium is the DFE. The green strategy leads to a low endemic equilibrium. The orange strategy leads either to an endemic equilibrium or to the extinction of the epidemic depending on the initial condition (Figure 7 b).

The benefit of the orange strategy over the purple one is its lower intensity. It comes along with the risk of the dynamics ending trapped at the endemic equilibrium if the initial condition is unfavourable, i.e. when NPI are set up too late (insert of Figure 7 b).

We set a threshold (here less than one case per 100,000) under which we consider that the epidemic has gone extinct. When the number of cases falls under this threshold, we assume that it is not necessary to maintain any NPI. The duration and the time evolution of NPI intensity is represented in Figure 7 c. The green strategy keeps the epidemic at low level: it requires a moderately intense but never ending NPI. Strategy 1 (blue, constant $\upsilon = 0.6$) is the most effective and has the shortest total NPI duration but may be difficult to implement from the start. It drives the epidemic to extinction in 39 days. It should be noticed that 0.6 already represents a high intensity NPI such as a lockdown, that may be difficult to set up in practice, or which at least requires some time to be achieved. For the same initial condition, NPI for purple and orange strategies last respectively 43 and 49 days. They have the advantage to propose NPI with a gradually increasing intensity that reaches the maximum value at the end of the epidemic, which gives health authorities more time to set it up. Overall, their duration seem reasonable compared to the one of the blue strategy.

Based on this findings, it seems more profitable to seek to get rid of the epidemic using a purple or orange strategy (Strategy 3). However, it may seem counter-intuitive in the sense that it is necessary to strengthen the NPI intensity as the number of infected decreases in order to achieve the eradication of the epidemic in some time frame. As shown in the previous section, most countries have adopted Strategy 1 (blue) or 2 (green) instead. When the health situation worsens, the level of measures is reinforced for some weeks in order to return to a lower level of virus circulation, resulting in successive epidemic waves. In France, three lockdowns have been established. For each lockdown, its intensity has been reduced when the epidemic peak has diminished sufficiently so as not to saturate the hospitals but without maintaining it long enough at a high level to bring about the eradication of the epidemic. These successive confinements have generated astronomical infectious and economic costs. Epidemic waves seem to endlessly followed each other unless a vaccination policy can achieve collective immunity.

To summarize, our results indicate that lockdowns should be strengthened and absolutely not released when the incidence drops, until the epidemic actually ends. Doing the contrary leads to a new increase of the number of cases towards an endemic equilibrium.

In our opinion, these epidemic control methods could be used locally for medium-sized cities that can be isolated for a period of at least one to two months by prohibiting or very strictly controlling the entry and exit of people from this city. The application of these classes of strategies would require the use of a significant number of tests allowing a good estimation of the numbers of infected people at the time when the control must be implemented. It requires to properly position the various endemic equilibria created by the epidemic control function. In the context of Covid 19, our work suggests that strong, short and early measures are more effective than mild but long-lasting ones. We think that those results may be of interest since some countries like Israel expect to live permanently with the disease.

7 | CONCLUSION

In this work, we studied a SEIRS epidemic model with reinfection and illustrated the results with an application to Covid-19 pandemic. We analyzed the effects of several kinds of infection-dependent NPIs on the dynamics of the epidemic and on the characteristics (existence and stability) of Disease Free and endemic equilibria. We showed that NPI strategies could be divided into three main classes, and highlighted their benefits and drawbacks, such as their ability to put an end to the epidemic, the amplitude and duration of the peaks and the feasibility of the considered measures. We found that constant NPI strategies are effective to extinguish the epidemic but may be too intense to be practically usable. Strategies with NPI intensity decreasing with

the number of cases I may also put an end to the epidemic by creating an Allee effect, while being easier to set up. However, they can lead to a large epidemic peak or a (lower) endemic equilibrium instead of extinction if they are not set up carefully. Finally, the most intuitive strategy (NPI intensity increasing with the number of cases) proved to be the least efficient while being unable to put an end to the epidemic.

Many countries decided to use strategies 1 or 2 against Covid-19, as we showed in Section 5. They have been reluctant to set high intensity NPIs at low virus circulation levels or during the early stages of the pandemic since doing so may have been greatly unpopular and a major restriction of liberties. However our work suggests that the final cost may have been reduced. Even if our results may be considered with care due to the many assumptions we made in our model, we think to have provided a good illustration that (1) delaying the response to a problem eventually results in a highest social and economical cost, and (2) people are nevertheless inclined to use that kind of sub-efficient strategy. We believe that such a conclusion holds for other major problems we are facing nowadays, in particular for the ones related to climate change.

As a perspective, we could study a network of several cities connected by the movement of individuals from one city to another by rail or by plane. It would be interesting to study the coupling of epidemic management methods depending on the number of infected people in the different cities. We refer to[54] and[55], for disease spread in meta-populations.

In the future, we plan to reconsider our model by considering two compartments for asymptomatic (A) and infectious (I) in a future SEAIRS version. However, we hope and we are inclined to think that our conclusions obtain through a theoretical approach on the effectiveness of the various strategies can be useful for practical case studies, as density dependent protection strategies could be used to target a sufficiently low level of endemicity or find a strategy to put an end to the epidemic while considering constraints such as social cost or hospitals capacity.

Conflict of interest

The authors declare no potential conflict of interests.

8 | FIGURES LIST

FIGURE 1 Reduction of the number of infections due to NPI. Infected individuals are represented in blue, and symptomatic/presymptomatic in orange. (a) Without NPI, four infections occur. (b) With NPI, a proportion $\upsilon = 0.5$ of individuals is isolated (shaded area). The number of infection is reduced to $(1-\upsilon)^2 = 0.25$ of the number of original number of infections.

FIGURE 2 Evolution of the epidemic in the absence of NPI $\upsilon = 0$, for $1/\gamma = 200$ (blue), 400 (green) and compared to a model without reinfection ($\gamma = 0$, red dashed curve). (a) active cases per 100,000 (b) and cumulative cases per 100,000. The initial conditions is $(S(0) = N-1, E(0) = 0, I(0) = 1)$. Parameters values are $\beta = 1.2$, $k = 0.27$, and $\alpha = 0.67$.

FIGURE 3 Comparison of constant control strategies: $\upsilon = 0.8$ (blue), $\upsilon = 0.5$ (orange), $\upsilon = 0.3$ (purple), $\upsilon = 0.2$ (green). Parameters values are $\beta = 1.2$, $k = 0.2$, $\alpha = 0.5$ and $\gamma = 1/200$, $N = 50{,}000{,}000$. The initial condition is I(0)=300 per 100,000. (a) comparison of functions υ and $\hat{\upsilon}$, with stable (solid circles) and unstable (empty circles) equilibria. (b) evolution of the number of active cases I. An insert show the details of the region $0 < t < 50$. (c) Evolution of the number of cumulative cases.

FIGURE 4 Comparison of strategies lowering the endemic equilibrium. Chosen functions are $\upsilon : I \mapsto \upsilon_0 I/(I+100)$, with $\upsilon_0 = 0.8$ (blue), $\upsilon_0 = 0.5$ (orange) and $\upsilon_0 = 0.3$ (purple). Parameters values are $\beta = 1.2$, $k = 0.2$, $\alpha = 0.5$ and $\gamma = 1/200$. The initial condition is I(0)=300 per 100,000 individuals. (a) comparison of functions υ and $\hat{\upsilon}$, with stable endemic equilibria (solid circles), and an unstable DFE (empty circle). (b) evolution of the number of active cases I per 100,000 individuals.

FIGURE 5 Comparison of control strategies which create an Allee effect. Chosen functions are piecewise linear maps, decreasing from 0.8 to 0 from $I = 0$ to $I = I_{max}$ and equal to 0 elsewhere, with $I_{max} = 300$ (blue), $I_{max} = 50$ (orange) and $I_{max} = 500$ (purple). Parameters values are $\beta = 1.2$, $k = 0.2$, $\alpha = 0.5$ and $\gamma = 1/200$, for a population of 50,000,000 individuals. The initial conditions is $S_0 = 60{,}000$, $E_0 = 800$, $I_0 = 100$ for 100,000 individuals. (a) comparison of functions υ and $\hat{\upsilon}$, with a stable (solid circle) DFE and unstable (empty circles) endemic equilibria. (b) evolution of the number of active cases I. The early dynamics is depicted in insert. (c) Phase portrait. Stable equilibria are represented by a solid sphere, and unstable equilibria by a diamond, in colors corresponding to their respective maps υ. Surfaces indicate the basin of attractions of the stable endemic equilibrium, the colors corresponding to their respective maps. The grey plane delimits the volume of possible initial conditions $(S + E + I + R \leq N)$.

FIGURE 6 Epidemiological dynamics and NPI strategies for UK, France, Germany and New-York City. Left: time evolution of the number of new cases, admission to hospitals, and NPI intensity ν. Middle: phase portrait of NPI intensity ν vs new cases. Right: phase portrait of NPI intensity ν vs hospitalizations. For each point clouds, a linear regression has been performed in order to see if a linear relationship could be exhibited.

FIGURE 7 Comparison of the different NPI strategies: constant control (blue), decreasing function (purple and orange) and lower endemic equilibrium (green). Parameters values are $\beta = 1.2$, $k = 0.2$, $\alpha = 0.5$ and $\gamma = 1/200$, for a population of 50,000,000 individuals. The initial conditions is $I(0) = 100$ per 100,000. (a) comparison of functions υ and $\hat{\upsilon}$, with stable (solid circles) and unstable (empty circles) equilibria. (b) evolution of the number of active cases I. Insert: an additional dynamic for the initial condition $S(0) = 45{,}000$, $E(0) = 200$, $I(0) = 800$ for the orange strategy. (c) NPI intensity $\upsilon(t)$.

FIGURE 8 Epidemiological dynamics and NPI strategies for different countries. Left: time evolution of the number of new cases, admission to hospitals, and NPI intensity ν. Right: phase portrait of NPI intensity ν vs new cases. For the point cloud, a linear regression has been performed in order to see if a linear relationship could be exhibited.

References

1. Allee Warder C, Bowen Edith S. Studies in animal aggregations: mass protection against colloidal silver among goldfishes. *Journal of Experimental Zoology.* 1932;61(2):185-207.
2. Odum Eugene Pleasants, Barrett Gary W. *Fundamentals of ecology*. Saunders Philadelphia; 1971.
3. Courchamp Franck, Berec Ludek, Gascoigne Joanna. *Allee effects in ecology and conservation*. OUP Oxford; 2008.
4. Holden M H, McDonald-Madden E. High prices for rare species can drive large populations extinct: the anthropogenic Allee effect revisited. *Journal of Theoretical Biology.* 2017;429:170-180.
5. Liu Yang, Gu Zhonglei, Xia Shang, et al. What are the underlying transmission patterns of COVID-19 outbreak? An age-specific social contact characterization. *EClinicalMedicine.* 2020;22:100354.
6. Xia Shang, Liu Jiming, Cheung William. Identifying the relative priorities of subpopulations for containing infectious disease spread. *PloS one.* 2013;8(6):e65271.
7. Perkins T Alex, Paz-Soldan Valerie A, Stoddard Steven T, et al. Calling in sick: impacts of fever on intra-urban human mobility. *Proceedings of the Royal Society B: Biological Sciences.* 2016;283(1834):20160390.
8. Auger Pierre, Moussaoui Ali. On the Threshold of Release of Confinement in an Epidemic SEIR Model Taking into Account the Protective Effect of Mask. *Bulletin of mathematical biology.* 2021;83(4):1–18.
9. Howard Jeremy, Huang Austin, Li Zhiyuan, et al. An evidence review of face masks against COVID-19. *Proceedings of the National Academy of Sciences.* 2021;118(4).
10. van den Driessche P., Watmough James. Reproduction numbers and sub-threshold endemic equilibria for compartmental models of disease transmission. *Mathematical Biosciences.* 2002;180(1):29-48.
11. Fehlberg E.. Klassische Runge-Kutta-Formeln vierter und niedrigerer Ordnung mit Schrittweiten-Kontrolle und ihre Anwendung auf Wärmeleitungsprobleme. *Computing.* 1970;6(1):61–71.
12. Shokri Ali, Mehdizadeh Khalsaraei Mohammad, Molayi Maryam. Nonstandard Dynamically Consistent Numerical Methods for MSEIR Model. *Journal of Applied and Computational Mechanics.* 2022;8(1):196-205.

13. Khalsaraei Mohammad Mehdizadeh, Shokri Ali, Ramos Higinio, Heydari Shahin. A positive and elementary stable non-standard explicit scheme for a mathematical model of the influenza disease. *Mathematics and Computers in Simulation (MATCOM).* 2021;182(C):397-410.

14. Kamrujjaman Md, Mahmud Md Shahriar, Ahmed Shakil, et al. SARS-CoV-2 and Rohingya Refugee Camp, Bangladesh: Uncertainty and How the Government Took Over the Situation. *Biology.* 2021;10(2):124. Number: 2 Publisher: Multidisciplinary Digital Publishing Institute.

15. Centers for Disease Control . . https://www.cdc.gov/nhsn/covid19/report-patient-impact.html2021.

16. Trentini Filippo, Marziano Valentina, Guzzetta Giorgio, et al. Pressure on the Health-Care System and Intensive Care Utilization During the COVID-19 Outbreak in the Lombardy Region of Italy: A Retrospective Observational Study in 43,538 Hospitalized Patients. *American Journal of Epidemiology.* 2021;191(1):137-146.

17. Antonini Chiara, Calandrini Sara, Stracci Fabrizio, Dario Claudio, Bianconi Fortunato. Mathematical Modeling and Robustness Analysis to Unravel COVID-19 Transmission Dynamics: The Italy Case. *Biology.* 2020;9(11):394.

18. Ota Miyo. Will we see protection or reinfection in COVID-19?. *Nature Reviews Immunology.* 2020;20(6):351–351.

19. Stokel-Walker Chris. What we know about covid-19 reinfection so far. *BMJ.* 2021;372.

20. Ward Helen, Cooke Graham, Atchison Christina, et al. Declining prevalence of antibody positivity to SARS-CoV-2: a community study of 365,000 adults. *medRxiv.* 2020;.

21. Callaway Ewen. Fast-spreading COVID variant can elude immune responses. *Nature.* 2021;589(7843):500–501.

22. Tillett Richard L, Sevinsky Joel R, Hartley Paul D, et al. Genomic evidence for reinfection with SARS-CoV-2: a case study. *The Lancet Infectious Diseases.* 2021;21(1):52–58.

23. Adam David. MODELLING THE PANDEMIC The simulations driving the world's response to COVID-19. *Nature.* 2020;580(7803):316–318.

24. Kissler Stephen M, Tedijanto Christine, Goldstein Edward, Grad Yonatan H, Lipsitch Marc. Projecting the transmission dynamics of SARS-CoV-2 through the postpandemic period. *Science.* 2020;368(6493):860–868.

25. Bacaër Nicolas. Un modèle mathématique des débuts de l'épidémie de coronavirus en France. *Mathematical Modelling of Natural Phenomena.* 2020;15:29.

26. Liu Zhihua, Magal Pierre, Seydi Ousmane, Webb Glenn. Understanding unreported cases in the COVID-19 epidemic outbreak in Wuhan, China, and the importance of major public health interventions. *Biology.* 2020;9(3):50.

27. Sun Haoxuan, Qiu Yumou, Yan Han, Huang Yaxuan, Zhu Yuru, Chen Song Xi. Tracking and predicting COVID-19 epidemic in China mainland. *medRxiv.* 2020;.

28. Kuniya Toshikazu. Prediction of the epidemic peak of coronavirus disease in Japan, 2020. *Journal of clinical medicine.* 2020;9(3):789.

29. Moussaoui Ali, Auger Pierre. Prediction of confinement effects on the number of COVID-19 outbreak in Algeria. *Mathematical Modelling of Natural Phenomena.* 2020;15:37.

30. Moussaoui Ali, Zerga El Hadi. Transmission dynamics of COVID-19 in Algeria: The impact of physical distancing and face masks. *AIMS Public Health.* 2020;7(4):816.

31. Kucharski Adam J, Klepac Petra, Conlan Andrew JK, et al. Effectiveness of isolation, testing, contact tracing, and physical distancing on reducing transmission of SARS-CoV-2 in different settings: a mathematical modelling study. *The Lancet Infectious Diseases.* 2020;20(10):1151–1160.

32. Tuite Ashleigh R, Fisman David N, Greer Amy L. Mathematical modelling of COVID-19 transmission and mitigation strategies in the population of Ontario, Canada. *Cmaj.* 2020;192(19):E497–E505.

33. Malkov Egor. Simulation of coronavirus disease 2019 (COVID-19) scenarios with possibility of reinfection. *Chaos, Solitons and Fractals.* 2020;139:110296.

34. Batistela Cristiane M., Correa Diego P.F., M Bueno , Piqueira José Roberto C.. SIRSi compartmental model for COVID-19 pandemic with immunity loss. *Chaos, Solitons and Fractals.* 2021;142:110388.

35. Costa Aratã Oliveira Cortez, Carvalho Aragão Neto Humberto, Lopes Nunes Ana Paula, Castro Ricardo, Almeida Reinaldo. COVID-19: Is reinfection possible?. *EXCLI Journal.* 2021;20:522–536.

36. Cai L, Liu J, Chen Y. Dynamics of an Age-Structured HIV Model with Super-Infection. *Applied and Computational Mathematics an International Journal.* 2021;20:257-276.

37. Sheehan Megan M., Reddy Anita J., Rothberg Michael B.. Reinfection Rates Among Patients Who Previously Tested Positive for Coronavirus Disease 2019: A Retrospective Cohort Study. *Clinical Infectious Diseases: An Official Publication of the Infectious Diseases Society of America.* 2021;73(10):1882–1886.

38. Hanrath Aidan T., Payne Brendan A. I., Duncan Christopher J. A.. Prior SARS-CoV-2 infection is associated with protection against symptomatic reinfection. *Journal of Infection.* 2021;82(4):e29–e30. Publisher: Elsevier.

39. Sabino Ester C et al.. Resurgence of COVID-19 in Manaus, Brazil, despite high seroprevalence. *Lancet.* 2021;397(10273):452-455.

40. Goddard Andrew F, Patel Mumtaz. SARS-CoV-2 variants and ending the COVID-19 pandemic. *Lancet.* 2021;397:952-954.

41. Hoffmann Markus, Krüger Nadine, Schulz Sebastian, et al. The Omicron variant is highly resistant against antibody-mediated neutralization: Implications for control of the COVID-19 pandemic. *Cell.* 2022;185(3):447-456.e11.

42. Ferguson N. *Report 49: Growth and immune escape of the Omicron SARS-CoV-2 variant of concern in England.* : Imperial College London; 2021.

43. Santé Publique France . . https://www.santepubliquefrance.fr/dossiers/coronavirus-covid-19/coronavirus-chiffres-cles-et-evolution-de-\la-covid-19-en-france-et-dans-le-monde/articles/covid-19-tableau-de-bord\-de-l-epidemie-en-chiffres2021.

44. Ma Qiuyue, Liu Jue, Liu Qiao, et al. Global Percentage of Asymptomatic SARS-CoV-2 Infections Among the Tested Population and Individuals With Confirmed COVID-19 Diagnosis: A Systematic Review and Meta-analysis. *JAMA Network Open.* 2021;4(12):e2137257-e2137257.

45. Johansson Michael A., Quandelacy Talia M., Kada Sarah, et al. SARS-CoV-2 Transmission From People Without COVID-19 Symptoms. *JAMA Network Open.* 2021;4(1):e2035057-e2035057.

46. Bender Jennifer K., Brandl Michael, Höhle Michael, Buchholz Udo, Zeitlmann Nadine. Analysis of Asymptomatic and Presymptomatic Transmission in SARS-CoV-2 Outbreak, Germany, 2020. *Emerging Infectious Diseases.* 2021;27(4):1159–1163.

47. Luo Lei, Liu Dan, Liao Xinlong, et al. Contact settings and risk for transmission in 3410 close contacts of patients with COVID-19 in Guangzhou, China: a prospective cohort study. *Annals of internal medicine.* 2020;173(11):879–887.

48. He Xi, Lau Eric HY, Wu Peng, et al. Temporal dynamics in viral shedding and transmissibility of COVID-19. *Nature medicine.* 2020;26(5):672–675.

49. Walsh Kieran A., Spillane Susan, Comber Laura, et al. The duration of infectiousness of individuals infected with SARS-CoV-2. *Journal of Infection.* 2020;81(6):847–856. Publisher: Elsevier.

50. Lauer Stephen A, Grantz Kyra H, Bi Qifang, et al. The incubation period of coronavirus disease 2019 (COVID-19) from publicly reported confirmed cases: estimation and application. *Annals of internal medicine.* 2020;172(9):577–582.

51. Hilton Joe, Keeling Matt J. Estimation of country-level basic reproductive ratios for novel Coronavirus (SARS-CoV-2/COVID-19) using synthetic contact matrices. *PLoS computational biology.* 2020;16(7):e1008031.

52. Ke Ruian, Romero-Severson Ethan, Sanche Steven, Hengartner Nick. Estimating the reproductive number R0 of SARS-CoV-2 in the United States and eight European countries and implications for vaccination. *Journal of Theoretical Biology.* 2021;517:110621.

53. Ferguson Neil M, Laydon Daniel, Nedjati-Gilani Gemma, et al. Impact of non-pharmaceutical interventions (NPIs) to reduce COVID-19 mortality and healthcare demand. Imperial College COVID-19 Response Team. *Imperial College COVID-19 Response Team.* 2020;:20.

54. Arino Julien, Van Den Driessche Pauline. The basic reproduction number in a multi-city compartmental epidemic model. In: Springer 2003 (pp. 135–142).

55. Arino Julien, Driessche P. Disease spread in metapopulations. *Fields Institute Communications.* 2006;48(1):1–13.

How to cite this article: Nguyen-Huu. T., Auger P., and Moussaoui A. (2022), On management strategies depending on the number of infected in order to stop a SEIRS epidemic: extinction of the epidemic by Allee effect, *Math Meth Appl Sci.*, *2022;00:xx–xx*.